forests

MDPI

Article

Chemical Recalcitrance Rather Than Soil Microbial Community Determined Short-Term Biochar Stability in a Poplar Plantation Soil

Fangchao Zhang, Weiwei Lu * and Fengjie Jin

Co-Innovation Center for Sustainable Forestry in Southern China, College of Ecology and Environment, Nanjing Forestry University, Nanjing 210037, China; zhangfc@njfu.edu.cn (F.Z.); jinfj@njfu.edu.cn (F.J.)
* Correspondence: wwlu@njfu.edu.cn

Abstract: The stability of biochar is fundamental to its soil carbon (C) sequestration potential. The relative importance of chemical recalcitrance and the soil microbial community on biochar stability is still unclear. To unveil the question, we conducted a 60-day incubation to explore the stability of two rice-straw-derived biochars pyrolyzed at 300 and 500 °C (denoted as BS300 and BS500), as well as the relative contribution of the soil microbial community and biochar chemical recalcitrance to biochar stability in a poplar plantation soil. Biochar-derived cumulative carbon dioxide (CO_2) emission was estimated to be 41.3 and 6.80 mg C kg^{-1}, accounting for 0.73 and 0.11% of the amended biochar-derived organic C (OC) in BS300 and BS500 treatments, respectively. The mean retention time (MRT) estimated by double-exponential model fitting was 49.4 years for BS300 and 231 years for BS500. Compared to control, BS300 and BS500 decreased β-D-glucosidase activity by 20.9 and 18.0%, while they decreased phenol oxidase activity by 31.8 and 18.9%, respectively. Furthermore, BS300 increased the soil microbial metabolic quotient (qCO_2) by 155%, but BS500 decreased it by 13.4%. In addition, BS300 resulted in a 520% higher biochar-derived hot-water-extractable OC than BS500. Partial least-squares path modeling (PLSPM) showed that the path efficients of biochar's chemical recalcitrance and microbial qCO_2 were 0.52 and 0.25, respectively, and that of the soil microbial activity is neglected. We conclude from this short-term study that chemical recalcitrance imposed a greater effect than soil microbial community on biochar stability.

Keywords: biochar; ^{13}C tracing; mean retention time; extracellular enzyme; chemical recalcitrance; microbial metabolic quotient

Citation: Zhang, F.; Lu, W.; Jin, F. Chemical Recalcitrance Rather Than Soil Microbial Community Determined Short-Term Biochar Stability in a Poplar Plantation Soil. *Forests* **2024**, *15*, 622. https://doi.org/10.3390/f15040622

Academic Editor: Azim Mallik

Received: 26 February 2024
Revised: 27 March 2024
Accepted: 28 March 2024
Published: 29 March 2024

1. Introduction

Biochar is a solid material produced by pyrolysis under limited or absent oxygen conditions. The unique properties of biochar, e.g., high carbon (C) and various nutrients, make it a potential measure to improve soil quality and increase yields [1–3]. In addition, biochar produced from raw plant material can sequester as high as 20% of net C from the atmosphere when compared to the fresh plant material, and, thus, is a carbon-negative material [4].

However, biochar can be mineralized into carbon dioxide (CO_2) through biotic and abiotic processes [5]. Carbon loss in biochar varied between 3 and 26% per 100 years, and the half-life of biochar can be between 10^2 and 10^7 years [6,7]. For example, the mean retention times (MRTs) were estimated to be 713 and 978 years for 450 and 550 °C wood (*Eucalyptus saligna* Sm.) biochars, respectively, following a 25-month incubation [8]. In contrast, the MRTs were estimated to be 62 and 100 years for 450 and 550 °C grass (*Astrebla* spp.) biochars, respectively, following a 120-day incubation [9]. The stability of biochar has been found to increase with an increasing pyrolysis temperature [10,11], primarily due to the more labile organic C (OC) such as alkanes contained in low-temperature biochars [12], and lower polarity and more aromatic compounds indicated by the lower O/C and H/C

ratios in high-temperature biochars [13]. Additionally, it has been observed that the type of feedstock (e.g., wood and herbaceous materials) significantly influences the stability of biochar, with herbaceous feedstocks being more susceptible to rapid biodegradation due to the higher content of labile organic matter in comparison to wood feedstocks [13].

Besides the small part of labile OC, such as water-soluble organics [2], biochar is primarily composed of aromatic C. It was reported that about 89.5% of the OC was aryl C as indicated by the ^{13}C NMR analysis [14]. Soil microbes utilize biochars by the secretion of a series of enzymes, particularly the oxidative enzymes responsible for the degradation of recalcitrant substances, such as lignins, tannins, and suberins [15,16]. Since the enzyme synthesis, transportation, and secretion are energy-intensive [17], soil micro-organisms prefer labile OC over recalcitrant OC contained in biochars due to the lower energy cost [18,19]. Following the uptake of biochar, soil microbes can respire biochar as CO_2 via catabolism; meanwhile, they can incorporate it into biomass via anabolism [10]. The trade-off of biochar-C partition between microbial catabolism and anabolism impacts the CO_2 flux derived from biochar. It was suggested that the highly labile C components in biochars were mineralized predominantly through biotic decomposition at the initial decomposition stage [20,21]. Some studies have emphasized the importance of intrinsic chemical recalcitrance in determining biochar stability in soils [22–24]. For example, Fang et al. (2014) investigated the stability of biochar pyrolyzed at 450 and 550 °C in four different soils and found that the relative proportions of alkyl and aromatic C in biochar and the degree of condensation of aromatic C were determinant factors affecting the biochar's stability in soil [22]. However, other studies have found that the soil microbial community has a pronounced effect on biochar stability [25–27]. Recent studies have found that the addition of biochar to ferralsol alters the preferential utilization of substrates by soil microbes, enhancing soil microbial diversity and leading to an increased biochar degradation [26]. Therefore, the relative importance of chemical recalcitrance and soil microbial activity in determining biochar stability is still illusive.

Here, we examined the decomposition dynamics of 300 °C and 500 °C biochars by conducting a 60-day incubation. We hypothesized that the biochar stability was primarily controlled by its chemical recalcitrance rather than the soil microbial community in the short term. The main objectives of this study were to (1) analyze the decomposition rate of two biochars in poplar plantation soils; and (2) determine the relative importance of the soil microbial community and biochar chemical recalcitrance influencing the biochar stability in soil.

2. Materials and Methods

2.1. Biochar Preparation and Characterization

The biochars used in this study were prepared from ^{13}C-labelled rice. Details regarding the ^{13}C labelling of rice, the production, and the properties of the biochars can be found in Lu et al. (2021) [14]. Briefly, the pulse labelling of rice was performed at the grain-filling stage of rice using $Ba^{13}CO_3$ (^{13}C 98 atom%). After being oven-dried and chopped into 3–5 cm pieces, the ^{13}C-labelled rice was pyrolyzed at temperature of 300 °C and 500 °C, respectively. To determine the $\delta^{13}C$ of OC, the biochar was first subjected to acid rinsing to remove inorganic C as described by Boutton et al. (1999) [28], and then analyzed using an isotope ratio mass spectrometer interfaced with an element analyzer (Flash EA-δV advantage, Thermo Fisher, Waltham, MA, USA) at Advanced Analysis and Testing Center, Nanjing Forestry University (AATU-NFU).

2.2. Soil Sampling and Characterization

Soil sample was collected from Dongtai Forest Farm (120°49′44″ E, 32°52′37″ N), Yancheng City, Jiangsu Province, China. The forest plantation, with an area of about 2000 hm^2, was established in 1965. It is located in the coastal area of the Yellow Sea, with an obvious monsoon climate, and the transition zone from temperate to north subtropical climate zone. This is a typical poplar plantation area in China, with a vegetation coverage

of about 85%, and mean annual temperature and precipitation of 13.7 °C and 1051 mm, respectively. The farm is part of the saline land of silting coastal area (alluvial soil) [29]. Soil in this area belongs to fluvisols according to the World Reference Base (WRB) [30].

A uniform poplar plantation was selected as the sampling site. The poplar plantation was established in 2012 and the soil sampling was conducted in October 2016. The understory vegetation in the plantation was composed of *Pteris biaurita* and *Humulus scandens* and the poplar species in the selected sampling site was *Populus deltoides* CL '35'. The afforestation planting space was 4 m × 6 m. Three plots (20 m × 20 m) were set up in the plantation, with the distance between adjacent plots no less than 5 m. Before soil sampling, plant residues and litter were removed. Six subsamples (0–20 cm) were collected from each plot, and a composite soil sample was obtained by mixing the six subsamples. Totally, three independent soil samples were prepared by mixing the subsamples. The soil samples were divided into two portions. One portion was stored at 4 °C used for the analysis of soil microbial biomass (MBC), and $\delta^{13}C$ of hot-water-extractable OC, as well as the incubation experiment within one week. The other portion was air-dried and used for analysis of basic physicochemical properties, which were as pH of 7.42, soil organ carbon (SOC) of 0.61%, and soil inorganic carbon (SIC) of 0.71%. The soil was determined as silt loam according to the USDA textural classification.

2.3. Incubation Experiment

We used three treatments: soil with no biochar amendment (control), soil amended with biochar pyrolyzed at 300 °C (BS300), and soil amended with biochar pyrolyzed at 500 °C (BS500). There are triplicates for each treatment. The soil sample and the biochar were crushed and passed through 2 mm and 0.25 mm sieves, respectively. Soil subsamples of 100 g (on an oven-dried basis) were weighted into designated 500 mL flasks. The biochar amendment rate was 1% (w/w), equivalent to a field application rate of 26 t ha^{-1} (20 cm soil depth, and soil bulk density of 1.30 g cm^{-3}). The soil was mixed uniformly with biochars. Deionized water was added to soils to bring the soil or soil–biochar mixture to 60% water-filled pore space (WFPS). The flasks were aerobically incubated at 25 °C in the dark. Soil water loss due to evaporation was supplemented using a pipette by weighing the flask every other day. Gases evolved from the flasks were periodically sampled on days 0, 1, 3, 7, 10, 45, and 60. The flasks were first purged with CO_2-free air, a 25 mL gas sample was immediately collected from the incubated flasks, followed by 25 mL nitrogen gas (N_2, 99.9999%) being refilled into the incubated flask to avoid negative pressure, and then another 25 mL gas samples were collected after 12 h enclosure. The CO_2 flux was calculated based on the concentration difference of gas sampled at time 0 and 12 h. To measure the soil extracellular enzyme activities and hot water-extractable OC content and $\delta^{13}C$, soils were collected on days 0, 1, 7, 30, and 60.

CO_2 concentration in the gas sample was analyzed by gas chromatograph (Agilent 7890B, Agilent, Santa Clara, CA, USA). CO_2-$\delta^{13}C$ was analyzed by isotope ratio mass spectrometer (Flash EA-δV advantage, Thermo Fisher, Waltham, MA, USA). Hot-water-extractable OC was analyzed according to Chodak et al. (2003) [31] and Landgraf et al. (2003) [32]: an aliquot of fresh soil (equivalent to 30 g oven-dried soil) was extracted with 150 mL (1:5 soil:water solution (w/v)) boiled deionized water for 1 h. After cooling, soil suspension was centrifuged at 2000 g for 10 min. The extracts were filtered through 0.45 µm filters, and was divided into two portions. One portion of filtrate was analyzed for hot-water-extractable OC content by Total Organic Carbon (TOC) Analyzer (Multi N/C 3000, Jena, Germany); the other portion was initially dried using a freeze-drier (FreeZone 2. L, Labconco, Kansas City, MO, USA), and then analyzed for hot-water-extractable OC-$\delta^{13}C$ using an isotope ratio mass spectrometer (Flash EA-δV advantage, Thermo Fisher, Waltham, MA, USA). Soil microbial biomass (MBC) was analyzed by chloroform fumigation–extraction method with the correction factor for calculation of 0.38. Soil microbial quotient was calculated as the CO_2 efflux divided by MBC.

2.4. Soil Extracellular Enzyme Activities

In this study, enzymes linked to the SOC decomposition process included β-D-glucosidase (EC 3.2.1.21), cellobiohydrolase (EC 3.2.1.91), phenol oxidase (EC 1.14.18.1), and laccase (EC 1.10.3.2). These enzymes are widely analyzed enzymes concerning carbon cycling [33], while laccase was specifically measured to further elucidate response of oxidase to biochar application in this study. Briefly, soil aliquots were extracted using 50 mM acetate buffer (pH = 5.0) with a 1:5 soil:liquid (w/v) to analyze β-D-glucosidase and cellobiohydrolase. We used p-nitrophenol (pNP)-β-D-glucopyranoside and pNP-cellobioside as substrates to analyzing the activities of soil β-D-glucosidase and cellobiohydrolase, respectively, and the modified methods followed those described by Sinsabaugh et al. (1994) [34] and Allison and Vitousek (2005) [17]. A spectrophotometer (UV-2550, Shimadzu, Kyoto, Japan) was used to measure the absorbance of the pNP assay at 410 nm following the incubation at 20 °C for 1 h in a dark incubator (MLR-351, Sanyo, Osaka, Japan). The soil phenol oxidase was determined using l-3, 4-dihydroxyphenylalanine (DOPA) as substrate, following Waldrop et al. (2000) [35] and Saiya-Cork et al. (2002) [36]. Tyrosine (Aladdin Co., Shanghai, China, ≥500 units mg^{-1} dry weight) was utilized to determine the extinction coefficient of the oxidized DOPA. Soil laccase was analyzed using 2, 2′-azinobis (3-ethylbenzothiazoline-6-sulphonic acid) (ABTS) as a substrate [37]. The extinction coefficient of the produced $ABTS^{+}$ was 36000 L mol^{-1} cm^{-1} [38]. The absorbance of the DOPA and ABTS assay was measured at 450 and 420 nm, respectively, using a microplate reader (Biolog, Hayward, CA, USA). Blank (without substrate) and control (without soil suspension) were simultaneously analyzed with triplicates for each enzyme. Enzyme activities were measured in triplicate, and the enzyme activity was expressed as μmol substrate converted g^{-1} dry soil h^{-1}.

2.5. Calculations

The ratio of the CO_2 efflux derived from biochar to total CO_2 efflux (f_b) is calculated using a two-component isotopic linear mixing model [39] as shown in Equation (1):

$$f_b = \frac{(\delta - \delta_s)}{(\delta_b - \delta_s)} \quad (1)$$

where δ (‰) is the $\delta^{13}C$ of CO_2 emitted from biochar-amended soils; δ_s (‰) is the $\delta^{13}C$ of native SOC; and δ_b (‰) is the $\delta^{13}C$ of OC in biochar. The $\delta^{13}C$ of CO_2 emitted from biochar-amended soil is calculated based on a mass balance equation [40] as shown in Equation (2):

$$\delta = \frac{(\delta_2 \times C_2 - \delta_1 \times C_1)}{(C_2 - C_1)} \quad (2)$$

where C_1 and C_2 are the concentration of CO_2 (μL L^{-1}), and δ_1 and δ_2 are the $\delta^{13}C$ of CO_2 (‰) in gases sampled immediately and 12 h after flask enclosure, respectively.

The quantity of native soil-derived hot-water-extractable OC in biochar-amended soils was calculated using the same method as that of native soil-derived CO_2 efflux (Equations (1) and (2)).

The course of biochar decomposition was estimated by fitting the biochar-derived CO_2 to a double-exponential model [9], and the formula is shown in Equation (3):

$$C_{Bt} = C \times \left(1 - e^{-k_1 t}\right) + (100 - C) \times \left(1 - e^{-k_2 t}\right) \quad (3)$$

where C_{Bt} (%) is the percentage of cumulatively mineralized biochar, t (d) is the incubation time, C (%) and $(100 - C)$ (%) is the percentage of relatively labile C and stable C, respectively, and k_1 (d^{-1}) and k_2 (d^{-1}) is the decomposition rate constant for labile C and stable C, respectively. The MRT is the inverse ($1/k_2$) of the decomposition rate constant.

2.6. Statistical Analysis

One-way ANOVA followed by LSD multiple comparison was conducted to examine the differences in biochar decomposition rate, cumulative biochar decomposition, and exocellular enzyme activities between the different treatments. An independent-sample *t* test was used to examine the difference of biochar-derived hot-water-extractable OC between BS300 and BS500 treatments. Significance was defined as $p < 0.05$. Statistical analysis was performed using SPSS 12.0. Graphs were generated using Origin 2018. A double-exponential model was used to fit the biochar decomposition rate using GraphPad 8.0.2. The effect of OC lability and microbial properties on biochar stability were assessed using partial least-squares path modeling (PLSPM) in the R package "plspm" [41].

3. Results

3.1. Soil Microbial Respiration, and Biochar-Derived CO_2 Efflux and Emission

Soil microbial respiration first decreased from day 0 to day 30, followed by a slight increase from day 30 to day 60 during incubation in all treatments (Figure 1a). Compared to control, BS500 had no influence on soil microbial respiration, while BS300 significantly increased it by 90% when averaged through incubation time (Figure 1a, $p < 0.05$). The biochar-derived CO_2 efflux peaked on day 0 (0.37 mg C kg^{-1} h^{-1}) and day 1 (0.05 mg C kg^{-1} h^{-1}) in the BS300 and BS500 treatments, respectively, followed by a sharp decrease until day 7 and subsequent slow decrease until the end of the incubation (Figure 1b). The biochar-derived cumulative CO_2 emission was estimated to be 41.3 and 6.80 mg C kg^{-1}, accounting for 0.73 and 0.11% of the amended biochar-OC in BS300 and BS500 treatments respectively (Figure 1c). The double-exponential model fitting showed that more than 99.6% of the OC contained in the studied biochars was recalcitrant. The MRT of 300 and 500 °C biochar was estimated to be 49.4 and 231 years, respectively (Table 1).

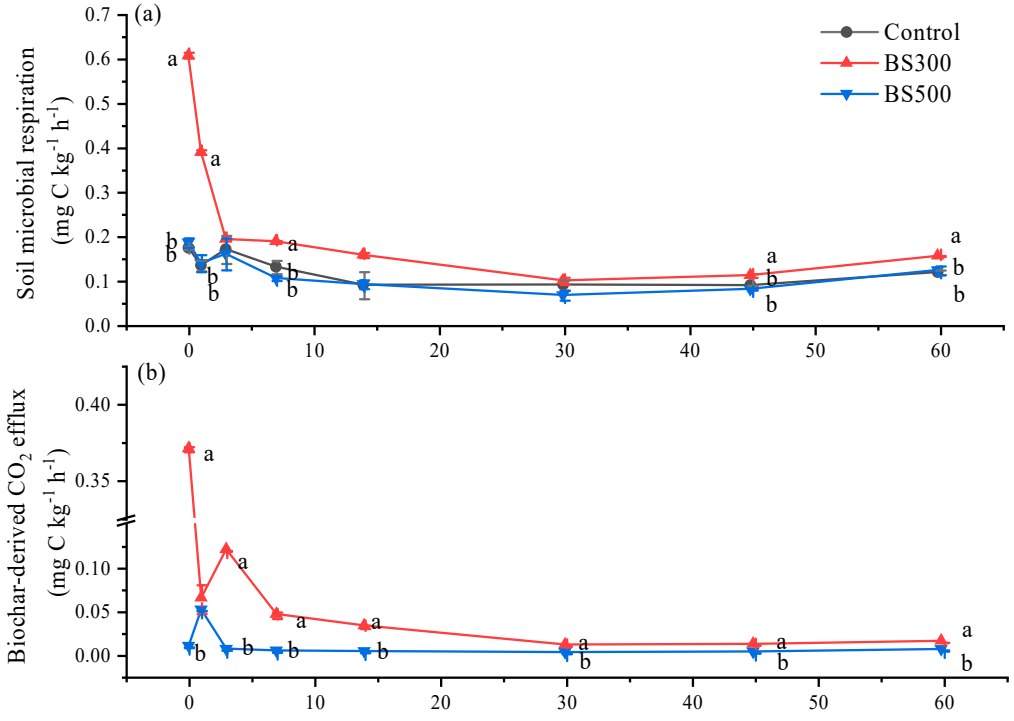

Figure 1. *Cont.*

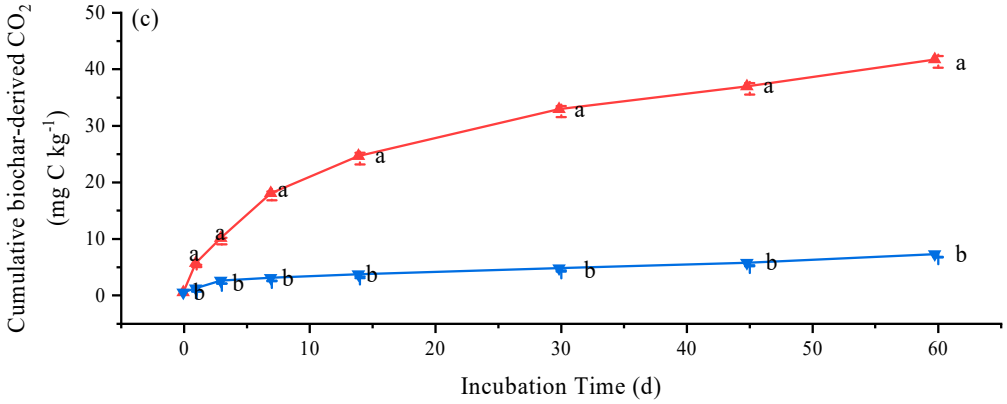

Figure 1. Temporal variations of microbial respiration (**a**), and carbon dioxide (CO_2) efflux (**b**) and cumulative emission (**c**) derived from biochars pyrolyzed at 300 °C (BS300) and 500 °C (BS500) amended to the poplar soil during 60 days of incubation. The different lowercase letters represent significant differences between treatments on the same incubation time ($p < 0.05$). The vertical error bars indicate the standard error ($n = 3$).

Table 1. Mean residence time and the proportions (%) of labile and recalcitrant fractions of biochars pyrolyzed at 300 °C (BS300) and 500 °C (BS500) amended to the soil estimated by fitting the cumulative mineralized biochar-C using a double-exponential model over 60 days of incubation [a].

Treatment	Labile C (%)	Recalcitrant (%)	Labile C (mg C kg^{-1})	Recalcitrant C (mg C kg^{-1})	MRT of Labile C (d)	MRT of Recalcitrant C (Year)	R^2
BS300	0.39 ± 0.02 [a,b]	99.61 ± 0.02 [b]	22.4 ± 0.95 [a]	5688 ± 0.95 [b]	6.01 ± 0.30 [a]	49.4 ± 0.68 [b]	0.998
BS500	0.03 ± 0.003 [b]	99.97 ± 0.003 [a]	2.09 ± 0.21 [b]	6268 ± 0.21 [a]	1.98 ± 0.19 [b]	231 ± 5.18 [a]	0.995

[a] Means ± standard errors ($n = 3$). [b] Different lowercase letters are significantly different at $p < 0.05$.

3.2. Soil Enzyme Activity

The examined soil enzyme activities initially decreased, then increased, and, finally, decreased during the incubation under BS300 and BS500 treatments (Figure 2). Both BS300 and BS500 changed the dynamic of the hydrolase (β-D-glucosidase and cellobiosidase) activity, showing little effect on the dynamic of oxidase (phenol oxidase and laccase) activity (Figure 2). When averaged through the incubation, compared to control, BS300 and BS500 decreased the β-D-glucosidase activity by 20.9 and 18.0% (Figure 2a), while they increased the cellobiosidase activity by 10.1 and 9.3%, respectively (Figure 2b), mainly occurring at the earlier incubation stage (days 0–7). Furthermore, BS300 and BS500 decreased the phenol oxidase activity by 31.8 and 18.9%, respectively (Figure 2c). There was no difference in the extracellular enzyme activities between BS300 and BS500 treatments (Figure 2).

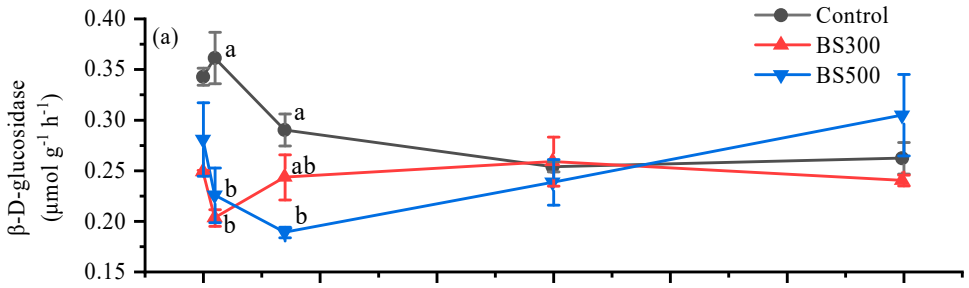

Figure 2. *Cont.*

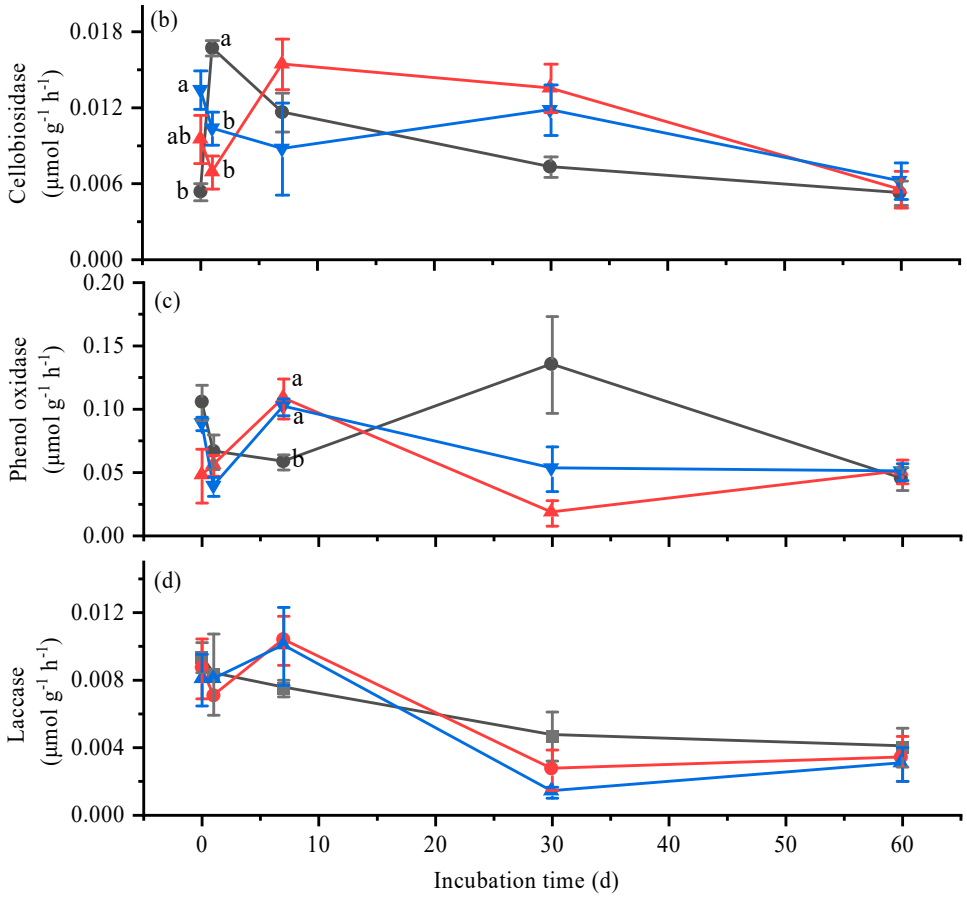

Figure 2. Temporal variations of β-D-glucosidase (**a**), cellobiosidase (**b**), laccase (**c**), and phenol oxidase (**d**) activity in soils without (Control) and with biochar pyrolyzed at 300 °C (BS300) and 500 °C (BS500) during 60 days of incubation. The different lowercase letters represent significant differences between treatments at the same incubation time ($p < 0.05$). The vertical error bars indicate the standard error ($n = 3$).

3.3. Soil Microbial Biomass and Metabolic Quotient

In general, soil microbial biomass was increased while the microbial metabolic quotient decreased during the incubation (Figure 3). Compared to control, BS300 and BS500 had no effect on soil microbial biomass except on days 0 and 1 (Figure 3a). BS300 increased the microbial metabolic quotient by 155.3%, while BS500 decreased it by 13.4%, following a 60-day incubation (Figure 3b).

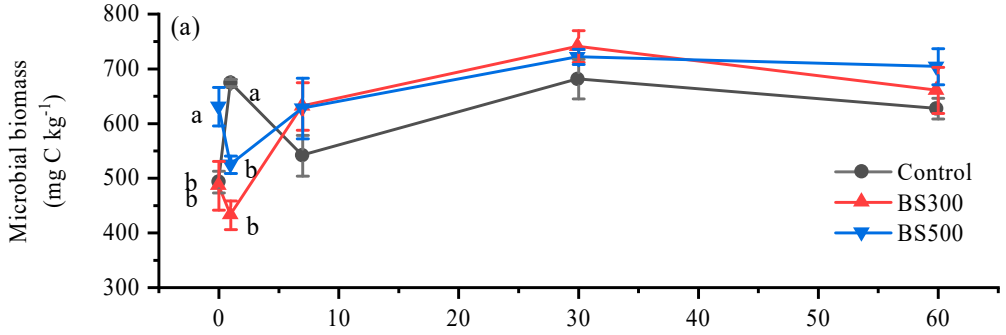

Figure 3. *Cont.*

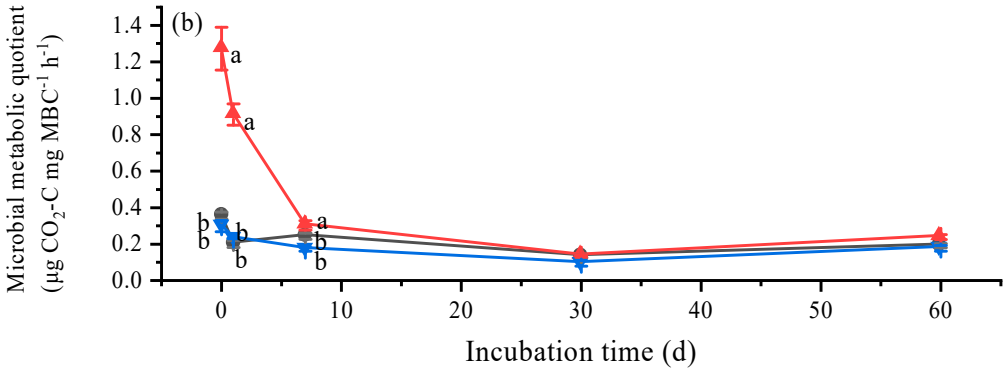

Figure 3. Temporal variations of microbial biomass (**a**) and metabolic quotient (**b**) in soils without (Control) and with biochar pyrolyzed at 300 °C (BS300) and 500 °C (BS500) during 60 days of incubation. The different lowercase letters represent significant differences between treatments on the same incubation time ($p < 0.05$). The vertical error bars indicate the standard error ($n = 3$).

3.4. Soil Hot-Water-Extractable OC

Soil hot-water-extractable OC fluctuated and remained relatively stable during the incubation; furthermore, it was not different among three treatments (Figure 4a). Biochar-derived hot-water-extractable OC peaked on day 0 (32.6 mg C kg^{-1}) and day 1 (5.36 mg C kg^{-1}) in the BS300 and BS500 treatments, respectively, and it gradually decreased during incubation (Figure 4b). When averaged through the incubation period, compared to control, BS300 and BS500 decreased biochar-derived hot-water-extractable OC by 42.1 and 80.3% after incubation. Furthermore, BS300 (24.0 mg C kg^{-1}) had a 520% higher biochar-derived hot-water-extractable OC than BS500 (3.87 mg C kg^{-1}).

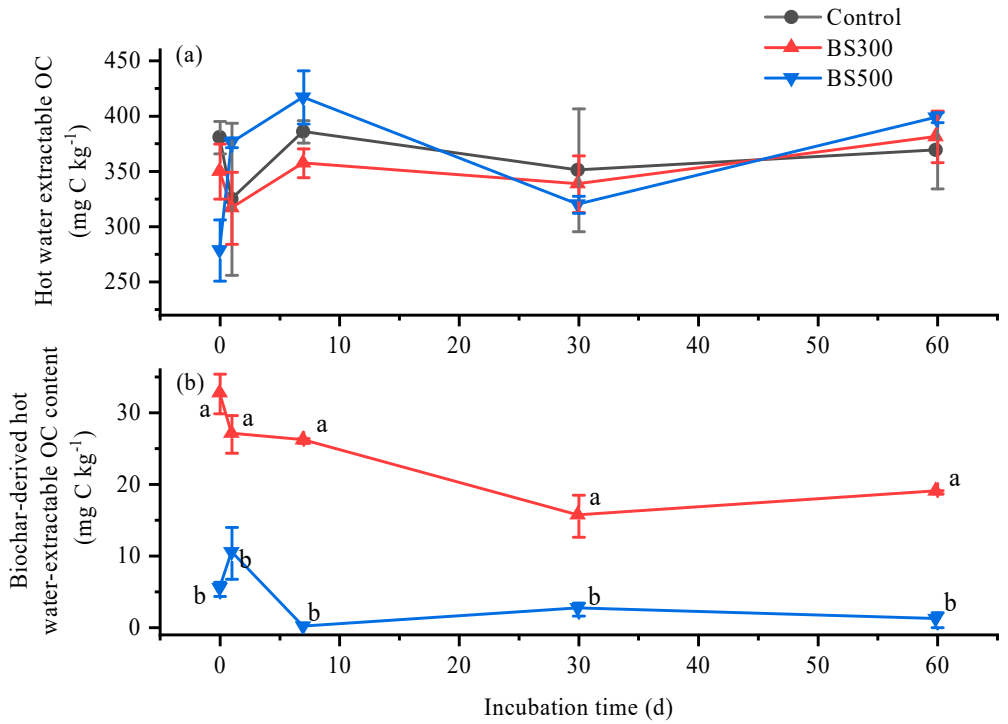

Figure 4. Temporal variations of the total (**a**), as well as biochar-derived (**b**), hot water-extractable organic carbon (OC) contents in soils with biochar pyrolyzed at 300 °C (BS300) and 500 °C (BS500) during 60 days of incubation. The different lowercase letters represent significant differences between treatments on the same incubation time ($p < 0.05$). The vertical error bars indicate the standard error ($n = 3$).

4. Discussion

4.1. The Stability of Biochars Pyrolyzed at Different Temperatures

In this study, 500 °C biochar was more stable than 300 °C biochar (Figure 1b), which was consistent with previous studies [18,42]. Biochar contains soluble, low-molecular-weight organics and recalcitrant aromatic compounds that mineralize at varying rates, and the relative proportions of these organic fractions in biochars vary upon the biochar's feedstock and pyrolysis temperature [23]. Compared with biochar pyrolyzed at lower temperatures, pyrolysis at higher temperatures lead to a higher aromatic C, higher degree of condensation of aromatic C, and less labile C in biochar [43], which may result in the greater stability of 500 °C biochar in soil.

The MRT of 300 °C and 500 °C biochar was estimated to be 49.4 and 231 years, respectively (Table 1), which was at the lower end of the previously reported MRTs [8,9,25,43–45] (Table 2). The differences in the MRTs of biochars could be attributed to differences in the properties of the used soil and biochar, as well as the incubation conditions [22,46]. The estimated MRT of biochars may increase due to the extension of the incubation time and depletion of labile C [23,45]. For example, the incubation time extended from 196 days to 3 years, and the estimated MRT of 550 °C leaf biochar in soil increased from 353 to 706 years [23]. Although recalcitrant C in biochar typically exhibits long-term persistence in soil [5], it is still depleted with increasing incubation time, which is probably attributed to the enhanced substrate availability. The enhanced substrate availability may be due to the shifts in microbial communities towards utilizing recalcitrant substrates following the exhaustion of labile C within the biochar [23,47]. Therefore, future studies should consider increasing the incubation time and determine potential factors contributing to the long-term decomposition of biochar. In addition, the MRTs of biochar estimated in laboratory incubations probably differ from those observed under field conditions, since our incubation experiments removed plant roots and litters from the soil. These plant residues might induce a co-metabolic with biochar, leading to a rapid decomposition of biochar-C under field conditions [10].

Table 2. Mean residence time of biochars in soils estimated by double first-order kinetics model.

Raw Material	Pyrolysis Temperature	Soil Type	Incubation Time (Day)	Experiment Type	MRT (Year)	Reference
Wood (*Eucalyptus salinga*)	450 °C and 550 °C	Vertisol	120	Laboratory	62~112 (450 °C) 100~248 (550 °C)	[9]
Wood (*Eucalyptus saligna*)	450 °C and 550 °C	Inceptisol, Entisol, Oxisol, Vertisol	365	Laboratory	44~259 (450 °C) 126~610 (550 °C)	[25]
Wood (*Eucalyptus saligna*)	450 °C and 550 °C	Inceptisol, Entisol, Oxisol, Vertisol	730	Laboratory	25~454 (450 °C) 93~1061 (550 °C)	[43]
Wood (*Eucalyptus saligna*)	450 °C	Arenosol, Cambisol, and Ferralsol	365	Field	44~1079 (Arenosol), 18~172 (Cambisol), and 11~29 (Ferralsol)	[44]
Rice straw	500 °C	Loamy, clay loam, and sand clay soils from plowing layers	390	Laboratory	618~2829	[45]
Wood (*Eucalyptus Salinga*)	450 °C and 550 °C	Vertisol	About 750	Laboratory	314~713 (450 °C) 567~978 (550 °C)	[8]

4.2. Biochar Stability as Related to Soil Microbial Community and OC Lability

In this study, BS300 and BS500 decreased β-D-glucosidase and phenol oxidase activities, but they had no significant effect on cellobiosidase and laccase activities (Figure 2a–c). In contrast, it was reported the amended biochar increased the soil phenol oxidase and β-D-glucosidase [48], and decreased soil cellobiosidase activity [49]. Extracellular enzyme activities, which depend on metabolic requirements and nutrient availability, were directly involved in the biodegradation of OC [50]. Since β-D-glucosidase activity is involved in the decomposition of labile C [51], the lower enzyme activity might indicate a higher C availability in the soil [14,52]. The decrease in soil β-D-glucosidase might be due to the phenolic compounds in biochars [53,54]. Moreover, the production of oxidase, i.e., phenol oxidase, and laccases is essential for the degradation of aromatic structures in biochar [55–57]. A two-year experiment has reported biochar-induced shifts in soil microbial communities to actinomycetes [58], as actinomycetes can utilize recalcitrant C in biochar through the production of oxidases [59]. In this study, it was observed that biochar did not increase the activity of oxidases (Figure 2a), possibly due to the absence of a shift of the microbial community to actinomycetes during the relatively short incubation period. The lack of a significant difference in the examined extracellular enzyme activities in the BS300 and BS500 treatments (Figure 2) indicated the different stabilities of 300 °C and 500 °C biochars were not primarily due to soil enzyme activity.

In our study, BS300 possessed the higher qCO_2 than BS500, primarily due to the higher CO_2 emission in BS300 treatment (Figure 3a,b). This result was consistent with previous studies [60,61]. The soil microbial community can modulate the organic matter turnover in mineral soils through the allocation of C they take up into anabolism and catabolism [62]. A high qCO_2 indicates that soil microbes allocate more C to respiration rather than growth. We found the qCO_2 was significantly correlated with the biochar decomposition rate ($r = 0.871$, $p < 0.01$, $n = 10$), which indicated that the soil microbial metabolic trait exerted a greater influence than soil enzyme activities on biochar decomposition. Similarly, Chen et al. (2018) [51] suggested soil microbial carbon use efficiency rather than enzyme activity determined native SOC decomposition.

Consistent with the biochar stability, the hot-water-extractable OC was higher in 300 °C biochar than 500 °C biochar (Figure 4), which was similar to a previous study [14]. Pyrogenic organic matter was believed to encompass a range of combustion products, from slightly charred biomass that may still be accessible for microbial degradation, to highly condensed refractory soot [63]. The labile C contained in 300 °C biochar might activate soil micro-organisms [60], which might, in turn, stimulate the biochar decomposition as indicated by the correlation between biochar-derived hot-water-extractable OC and biochar decomposition rate.

The results of partial least-squares path modeling (PLSPM) indicated that chemical recalcitrance exerted a greater influence than the soil microbial community on biochar stability (Figure 5), which aligned with our initial hypothesis. Our result was consistent with a recent study which proposed that the OC fraction of biochar was more important than the microbial activity and viability in the determination of biochar OC oxidation through a 119-day incubation [12]. Similarly, Bamminger et al. (2014) [54] found that the biochar properties, especially the OC content, had a greater influence on its stability than the soil properties in a 57-day incubation. Although it has been reported that microbial metabolism and enzyme activities can influence the decomposition of biochar [58], the chemical recalcitrance of the carbon in biochar is the most important factor affecting the stability of biochar. Long-term incubation studies and field studies are required to obtain realistic estimates of biochar stability in mineral soils. Soil properties, such as pH, SOC, and clay content, are important factors affecting biochar stability [22].

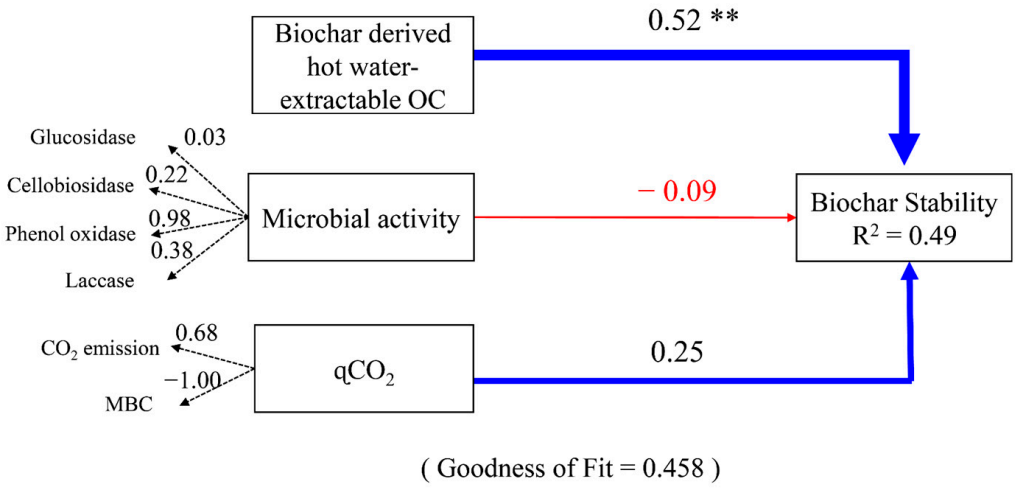

Figure 5. Partial least-squares path model (PLS-PM) illustrating the effects of soil microbial activity, metabolic quotient (qCO_2), and biochar-derived hot-water-extractable organic carbon (OC) on biochar stability in soils. The path coefficients are calculated after 1000 bootstraps and are reflected in the width of the arrows, with blue and red arrows indicating positive and negative effects, respectively. The path coefficients indicated by ** represent significant difference from 0 at $p < 0.01$. R^2 indicates the proportion of variance explained for the latent variable of biochar stability. The numbers on the dashed arrows are the loading scores of the observed variables that create the latent variables. The PLS-PM is assessed using the Goodness of Fit statistic (0.458). CO_2 and MBC represent carbon dioxide and soil microbial biomass carbon, respectively.

5. Conclusions

In this study, the effects of chemical recalcitrance and the soil microbial community on the stability of biochars in an alkaline plantation soil were explored in a 60-day incubation by using the ^{13}C tracing technique and PLS-PM analysis. The MRT of biochar pyrolyzed at 300 and 500 °C in the studied soil was estimated to be 49.4 and 231 years, respectively. PLS-PM analysis indicated that hot-water-extractable OC was the most important factor influencing the biochar decomposition rate. This study provides empirical evidence that the chemical recalcitrance of biochar has a greater influence on its stability than the soil microbial community in the short term. Further studies should examine the applicability of our finding in other soil types and under field conditions.

Author Contributions: Conceptualization, W.L.; software, F.Z. and W.L.; investigation, W.L. and F.Z.; validation, F.Z. and W.L.; data curation, W.L. and F.Z.; writing—original draft preparation, F.Z.; writing—review and editing, W.L.; visualization, F.Z. and W.L.; supervision, W.L. and F.J.; funding acquisition, W.L. All authors have read and agreed to the published version of the manuscript.

Funding: This study was funded by the National Natural Science Foundation of China (41701264), Natural Science Foundation of Huaian City, Jiangsu Province of China (HAB202164), and Postgraduate Research & Practice Innovation Program of Jiangsu Province (KYCX23_1126).

Data Availability Statement: All data generated and analyzed during the current study are available from the corresponding author upon reasonable request.

Acknowledgments: We are grateful for the assistance of the Advanced Analysis and Testing Center, Nanjing Forestry University (AATU-NFU). We also thank the other members of our team for their assistance in the laboratory experiments.

Conflicts of Interest: The authors declare no conflicts of interest.

References

1. Agegnehu, G.; Srivastava, A.K.; Bird, M.I. The role of biochar and biochar-compost in improving soil quality and crop performance: A review. *Appl. Soil Ecol.* **2017**, *119*, 156–170. [CrossRef]
2. Bakshi, S.; Banik, C.; Laird, D.A. Quantification and characterization of chemically-and thermally-labile and recalcitrant biochar fractions. *Chemosphere* **2018**, *194*, 247–255. [CrossRef] [PubMed]
3. Fan, Q.Y.; Sun, J.X.; Chu, L.; Cui, L.Q.; Quan, G.X.; Yan, J.L.; Hussain, Q.; Iqbal, M. Effects of chemical oxidation on surface oxygen-containing functional groups and adsorption behavior of biochar. *Chemosphere* **2018**, *207*, 33–40. [CrossRef] [PubMed]
4. Lehmann, J. A handful of carbon. *Nature* **2007**, *447*, 143–144. [CrossRef] [PubMed]
5. Zimmerman, A.R.; Gao, B.; Ahn, M. Positive and negative carbon mineralization priming effects among a variety of biochar-amended soils. *Soil Biol. Biochem.* **2011**, *43*, 1169–1179. [CrossRef]
6. Sohi, S.P.; Krull, E.; Lopez-Capel, E.; Bol, R. A review of biochar and its use and function in soil. In *Advances in Agronomy*; Sparks, D.L., Ed.; Academic Press: Cambridge, MA, USA, 2010; pp. 47–82.
7. Zimmerman, A.R. Abiotic and microbial oxidation of laboratory-produced black carbon (biochar). *Environ. Sci. Technol.* **2010**, *44*, 1295–1301. [CrossRef]
8. Fang, Y.; Singh, B.P.; Nazaries, L.; Keith, A.; Tavakkoli, E.; Wilson, N.; Singh, B. Interactive carbon priming, microbial response and biochar persistence in a vertisol with varied inputs of biochar and labile organic matter. *Eur. J. Soil Sci.* **2019**, *70*, 960–974. [CrossRef]
9. Keith, A.; Singh, B.; Singh, B.P. Interactive priming of biochar and labile organic matter mineralization in a smectite-rich soil. *Environ. Sci. Technol.* **2011**, *45*, 9611–9618. [CrossRef]
10. Ameloot, N.; Graber, E.R.; Verheijen, F.G.A.; De Neve, S. Interactions between biochar stability and soil organisms: Review and research needs. *Eur. J. Soil Sci.* **2013**, *64*, 379–390. [CrossRef]
11. Yang, Y.; Sun, K.; Han, L.F.; Chen, Y.L.; Liu, J.; Xing, B.S. Biochar stability and impact on soil organic carbon mineralization depend on biochar processing, aging and soil clay content. *Soil Biol. Biochem.* **2022**, *169*, 108657. [CrossRef]
12. Chen, G.; Wang, X.; Zhang, R. Decomposition temperature sensitivity of biochars with different stabilities affected by organic carbon fractions and soil microbes. *Soil Tillage Res.* **2019**, *186*, 322–332. [CrossRef]
13. Ghorbani, M.; Konvalina, P.; Neugschwandtner, R.W.; Soja, G.; Bárta, J.; Chen, W.; Amirahmadi, E. How do different feedstocks and pyrolysis conditions effectively change biochar modification scenarios? A critical analysis of engineered biochars under H_2O_2 oxidation. *Energy Convers. Manag.* **2024**, *300*, 117924. [CrossRef]
14. Lu, W.; Zha, Q.; Zhang, H.; Chen, H.Y.H.; Yu, J.; Tu, F.; Ruan, H. Changes in soil microbial communities and priming effects induced by rice straw pyrogenic organic matter produced at two temperatures. *Geoderma* **2021**, *400*, 115217. [CrossRef]
15. Baldrian, P. Fungal laccases-occurrence and properties. *FEMS Microbiol. Rev.* **2006**, *30*, 215–242. [CrossRef] [PubMed]
16. Blagodatskaya, E.; Kuzyakov, Y. Mechanisms of real and apparent priming effects and their dependence on soil microbial biomass and community structure: Critical review. *Biol. Fert. Soils* **2008**, *45*, 115–131. [CrossRef]
17. Allison, S.D.; Vitousek, P.M. Responses of extracellular enzymes to simple and complex nutrient inputs. *Soil Biol. Biochem.* **2005**, *37*, 937–944. [CrossRef]
18. Han, L.; Sun, K.; Yang, Y.; Xia, X.; Li, F.; Yang, Z.; Xing, B. Biochar's stability and effect on the content, composition and turnover of soil organic carbon. *Geoderma* **2020**, *364*, 114184. [CrossRef]
19. Sackett, T.E.; Basiliko, N.; Noyce, G.L.; Winsborough, C.; Schurman, J.; Ikeda, C.; Thomas, S.C. Soil and greenhouse gas responses to biochar additions in a temperate hardwood forest. *GCB Bioenergy* **2015**, *7*, 1062–1074. [CrossRef]
20. Bruun, S.; Luxhoi, J. Is biochar production really carbon-negative? *Environ. Sci. Technol.* **2008**, *42*, 1388. [CrossRef]
21. Wang, J.; Xiong, Z.; Kuzyakov, Y. Biochar stability in soil: Meta-analysis of decomposition and priming effects. *GCB Bioenergy* **2016**, *8*, 512–523. [CrossRef]
22. Fang, Y.; Singh, B.; Singh, B.P.; Krull, E. Biochar carbon stability in four contrasting soils. *Eur. J. Soil Sci.* **2014**, *65*, 60–71. [CrossRef]
23. Singh, B.P.; Cowie, A.L.; Smernik, R.J. Biochar carbon stability in a clayey soil as a function of feedstock and pyrolysis temperature. *Environ. Sci. Technol.* **2012**, *46*, 11770–11778. [CrossRef] [PubMed]
24. Chao, L.; Zhang, W.D.; Wang, S.L. Understanding the dominant controls on biochar decomposition using boosted regression trees. *Eur. J. Soil Sci.* **2018**, *69*, 512–520. [CrossRef]
25. Andrés, P.; Rosell-Melé, A.; Colomer-Ventura, F.; Denef, K.; Cotrufo, M.F.; Riba, M.; Alcañiz, J.M. Belowground biota responses to maize biochar addition to the soil of a mediterranean vineyard. *Sci. Total Environ.* **2019**, *660*, 1522–1532. [CrossRef]
26. Sheng, Y.; Zhu, L. Biochar alters microbial community and carbon sequestration potential across different soil ph. *Sci. Total Environ.* **2018**, *622–623*, 1391–1399. [CrossRef] [PubMed]
27. Zhang, H.; Wang, S.; Zhang, J.; Tian, C.; Luo, S. Biochar application enhances microbial interactions in mega-aggregates of farmland black soil. *Soil Tillage Res.* **2021**, *213*, 105145. [CrossRef]
28. Boutton, T.W.; Archer, S.R.; Midwood, A.J. Stable isotopes in ecosystem science: Structure, function and dynamics of a subtropical savanna. *Rapid Commun. Mass. Spectrom.* **1999**, *13*, 1263–1277. [CrossRef]
29. Ge, Z.; Fang, S.; Chen, H.; Zhu, R.; Peng, S.; Ruan, H. Soil aggregation and organic carbon dynamics in poplar plantations. *Forests* **2018**, *9*, 508. [CrossRef]

30. Ren, T.; Yu, X.; Liao, J.; Du, Y.; Zhu, Y.; Jin, L.; Wang, B.; Xu, H.; Xiao, W.; Chen, H.Y.H.; et al. Application of biogas slurry rather than biochar increases soil microbial functional gene signal intensity and diversity in a poplar plantation. *Soil Biol. Biochem.* **2020**, *146*, 107825. [CrossRef]
31. Chodak, M.; Khanna, P.; Beese, F. Hot water extractable c and n in relation to microbiological properties of soils under beech forests. *Biol. Fert. Soils* **2003**, *39*, 123–130. [CrossRef]
32. Landgraf, D.; Boehm, C.; Makeschin, F. Dynamic of different c and n fractions in a cambisol under five year succession fallow in saxony (Germany). *J. Plant Nutr. Soil Sci.* **2003**, *166*, 319–325. [CrossRef]
33. Sinsabaugh, R.L.; Lauber, C.L.; Weintraub, M.N.; Ahmed, B.; Allison, S.D.; Crenshaw, C.; Contosta, A.R.; Cusack, D.; Frey, S.; Gallo, M.E.; et al. Stoichiometry of soil enzyme activity at global scale. *Ecol. Lett.* **2008**, *11*, 1252–1264. [CrossRef] [PubMed]
34. Sinsabaugh, R.L.; Osgood, M.P.; Findlay, S. Enzymatic models for estimating decomposition rates of particulate detritus. *J. N. Am. Benthol. Soc.* **1994**, *13*, 160–169. [CrossRef]
35. Waldrop, M.P.; Balser, T.C.; Firestone, M.K. Linking microbial community composition to function in a tropical soil. *Soil Biol. Biochem.* **2000**, *32*, 1837–1846. [CrossRef]
36. Saiya-Cork, K.R.; Sinsabaugh, R.L.; Zak, D.R. The effects of long term nitrogen deposition on extracellular enzyme activity in an acer saccharum forest soil. *Soil Biol. Biochem.* **2002**, *34*, 1309–1315. [CrossRef]
37. Floch, C.; Alarcon-Gutiérrez, E.; Criquet, S. Abts assay of phenol oxidase activity in soil. *J. Microbiol. Meth.* **2007**, *71*, 319–324. [CrossRef] [PubMed]
38. Artz, R.R.E.; Reid, E.; Anderson, I.C.; Campbell, C.D.; Cairney, J.W.G. Long term repeated prescribed burning increases evenness in the basidiomycete laccase gene pool in forest soils. *FEMS Microbiol. Ecol.* **2009**, *67*, 397–410. [CrossRef] [PubMed]
39. Amelung, W.; Brodowski, S.; Sandhage-Hofmann, A.; Bol, R. *Combining Biomarker with Stable Isotope Analyses for Assessing the Transformation and Turnover of Soil Organic Matter*; Sparks, D.L., Ed.; Academic Press: Cambridge, MA, USA, 2008; pp. 155–250.
40. Balesdent, J.; Mariotti, A.; Boutton, T.W.; Yamasaki, S.I. Measurement of soil organic matter turnover using ^{13}C natural abundance. In *Mass Spectrometry of Soils*; Marcel Dekker: New York, NY, USA, 1996.
41. Wagg, C.; Bender, S.F.; Widmer, F.; van der Heijden, M.G.A. Soil biodiversity and soil community composition determine ecosystem multifunctionality. *Proc. Natl. Acad. Sci. USA* **2014**, *111*, 5266–5270. [CrossRef] [PubMed]
42. Kumar, M.R.; Jaya, P.K.D.; Narula, A.; Minnat, C.S.; Ullhas, N.S. Production and beneficial impact of biochar for environmental application: A review on types of feedstocks, chemical compositions, operating parameters, techno-economic study, and life cycle assessment. *Fuel* **2023**, *343*, 127968. [CrossRef]
43. Fang, Y.; Singh, B.; Singh, B.P. Effect of temperature on biochar priming effects and its stability in soils. *Soil Biol. Biochem.* **2015**, *80*, 136–145. [CrossRef]
44. Singh, B.P.; Fang, Y.; Boersma, M.; Collins, D.; Van Zwieten, L.; Macdonald, L.M. In situ persistence and migration of biochar carbon and its impact on native carbon emission in contrasting soils under managed temperate pastures. *PLoS ONE* **2015**, *10*, e141560. [CrossRef]
45. Wu, M.; Han, X.; Zhong, T.; Yuan, M.; Wu, W. Soil organic carbon content affects the stability of biochar in paddy soil. *Agric. Ecosyst. Environ.* **2016**, *223*, 59–66. [CrossRef]
46. Wang, X.; Song, D.; Liang, G.; Zhang, Q.; Ai, C.; Zhou, W. Maize biochar addition rate influences soil enzyme activity and microbial community composition in a fluvo-aquic soil. *Appl. Soil Ecol.* **2015**, *96*, 265–272. [CrossRef]
47. van Bergeijk, D.A.; Terlouw, B.R.; Medema, M.H.; van Wezel, G.P. Ecology and genomics of actinobacteria: New concepts for natural product discovery. Nature reviews. *Microbiology* **2020**, *18*, 546–558. [CrossRef]
48. Budai, A.; Rasse, D.P.; Lagomarsino, A.; Lerch, T.Z.; Paruch, L. Biochar persistence, priming and microbial responses to pyrolysis temperature series. *Biol. Fert. Soils* **2016**, *52*, 749–761. [CrossRef]
49. Khadem, A.; Raiesi, F. Influence of biochar on potential enzyme activities in two calcareous soils of contrasting texture. *Geoderma* **2017**, *308*, 149–158. [CrossRef]
50. Caldwell, B.A. Enzyme activities as a component of soil biodiversity: A review. *Pedobiologia* **2005**, *49*, 637–644. [CrossRef]
51. Chen, L.; Liu, L.; Mao, C.; Qin, S.; Wang, J.; Liu, F.; Blagodatsky, S.; Yang, G.; Zhang, Q.; Zhang, D.; et al. Nitrogen availability regulates topsoil carbon dynamics after permafrost thaw by altering microbial metabolic efficiency. *Nat. Commun.* **2018**, *9*, 3951. [CrossRef]
52. Jain, S.; Mishra, D.; Khare, P.; Yadav, V.; Deshmukh, Y.; Meena, A. Impact of biochar amendment on enzymatic resilience properties of mine spoils. *Sci. Total Environ.* **2016**, *544*, 410–421. [CrossRef]
53. Min, K.; Freeman, C.; Kang, H.; Choi, S. The regulation by phenolic compounds of soil organic matter dynamics under a changing environment. *Biomed. Res. Int.* **2015**, *2015*, 825098. [CrossRef]
54. Bamminger, C.; Marschner, B.; Jüschke, E. An incubation study on the stability and biological effects of pyrogenic and hydrothermal biochar in two soils. *Eur. J. Soil Sci.* **2014**, *65*, 72–82. [CrossRef]
55. Atkinson, C.J.; Fitzgerald, J.D.; Hipps, N.A. Potential mechanisms for achieving agricultural benefits from biochar application to temperate soils: A review. *Plant Soil* **2010**, *337*, 1–18. [CrossRef]
56. Hockaday, W.C. The Organic Geochemistry of Charcoal Black Carbon in the Soils of the University of Michigan Biological Station. Ph.D. Thesis, Ohio State University, Columbus, OH, USA, 2006.
57. Hofrichter, M.; Ziegenhagen, D.; Sorge, S.; Ullrich, R.; Bublitz, F.; Fritsche, W. Degradation of lignite (low-rank coal) by ligninolytic basidiomycetes and their manganese peroxidase system. *Appl. Microbiol. Biotechnol.* **1999**, *52*, 78–84. [CrossRef]

58. Song, D.; Chen, L.; Zhang, S.; Zheng, Q.; Ullah, S.; Zhou, W.; Wang, X. Combined biochar and nitrogen fertilizer change soil enzyme and microbial activities in a 2-year field trial. *Eur. J. Soil Biol.* **2020**, *99*, 103212. [CrossRef]
59. Blagodatskaya, E.V.; Blagodatsky, S.A.; Anderson, T.H.; Kuzyakov, Y. Contrasting effects of glucose, living roots and maize straw on microbial growth kinetics and substrate availability in soil. *Eur. J. Soil Sci.* **2009**, *60*, 186–197. [CrossRef]
60. Lévesque, V.; Rochette, P.; Ziadi, N.; Dorais, M.; Antoun, H. Mitigation of CO_2, CH_4 and N_2O from a fertigated horticultural growing medium amended with biochars and a compost. *Appl. Soil Ecol.* **2018**, *126*, 129–139. [CrossRef]
61. Zhou, H.; Zhang, D.; Wang, P.; Liu, X.; Cheng, K.; Li, L.; Zheng, J.; Zhang, X.; Zheng, J.; Crowley, D.; et al. Changes in microbial biomass and the metabolic quotient with biochar addition to agricultural soils: A meta-analysis. *Agric. Ecosyst. Environ.* **2017**, *239*, 80–89. [CrossRef]
62. Schimel, J.P.; Schaeffer, S.M. Microbial control over carbon cycling in soil. *Front. Microbiol.* **2012**, *3*, 31913. [CrossRef] [PubMed]
63. Masiello, C.A. New directions in black carbon organic geochemistry. *Mar. Chem.* **2004**, *92*, 201–213. [CrossRef]